

# Dynamic or Nondynamic? Helical Trajectory in Hexabenzocoronene Nanotubes Biased by a Detachable Chiral Auxiliary

Wei Zhang,<sup>†,‡</sup> Wusong Jin,<sup>§</sup> Takanori Fukushima,<sup>\*,||</sup> Noriyuki Ishii,<sup>⊥</sup> and Takuzo Aida<sup>\*,†,‡</sup>

<sup>†</sup>RIKEN Advanced Science Institute, 2-1 Hirosawa, Wako, Saitama 351-0198, Japan

<sup>‡</sup>Department of Chemistry and Biotechnology, School of Engineering, The University of Tokyo, 7-3-1 Hongo, Bunkyo-ku, Tokyo 113-8656, Japan

<sup>§</sup>College of Chemistry, Chemical Engineering and Biotechnology, Donghua University, 2999 North Renmin Road, Songjiang, Shanghai 201620, P. R. China

<sup>||</sup>Chemical Resources Laboratory, Tokyo Institute of Technology, 4259 Nagatsuta, Midori-ku, Yokohama 226-8503, Japan

<sup>⊥</sup>Biological Information Research Center, National Institute of Advanced Industrial Science and Technology (AIST), Tsukuba Central-6, 1-1-1 Higashi, Tsukuba, Ibaraki 305-8566, Japan

## Supporting Information

**ABSTRACT:** When ether vapor was allowed to diffuse into a CH<sub>2</sub>Cl<sub>2</sub> solution of an enantiomer of a hexa-*peri*-hexabenzocoronene (HBC) derivative carrying a chiral (BINAP)Pt(II)-appended coordination metallacycle (HBC<sup>Py</sup><sub>[(R)-Pt]</sub> or HBC<sup>Py</sup><sub>[(S)-Pt]</sub>), screw-sense-selective assembly took place to give optically active nanotubes (NT<sup>Py</sup><sub>[(R)-Pt]</sub> or NT<sup>Py</sup><sub>[(S)-Pt]</sub>) with helical chirality, which were enriched in either left-handed (*M*)-NT<sup>Py</sup><sub>[(R)-Pt]</sub> or right-handed (*P*)-NT<sup>Py</sup><sub>[(S)-Pt]</sub>, depending on the absolute configuration of the (BINAP)Pt(II) pendant. When MeOH was used instead of ether for the vapor-diffusion-induced assembly, nanocoils formed along with the nanotubes. As determined by scanning electron microscopy, the diastereomeric excess of the nanocoils was 60% (80:20 diastereomeric ratio). Removal of the (BINAP)Pt(II) pendants from NT<sup>Py</sup><sub>[(R)-Pt]</sub> or NT<sup>Py</sup><sub>[(S)-Pt]</sub> with ethylenediamine yielded metal-free nanotubes (NT<sup>Py</sup>) that remained optically active even upon heating without any change in the circular dichroism spectral profile. No helical inversion took place when NT<sup>Py</sup> derived from HBC<sup>Py</sup><sub>[(R)-Pt]</sub> or HBC<sup>Py</sup><sub>[(S)-Pt]</sub> was allowed to complex with (BINAP)Pt(II) with an absolute configuration opposite to the original one.

In general, the formation of large, elaborate organic nanostructures with well-defined molecular geometries has been considered to require that the assembly process carries sufficiently high thermodynamic reversibility.<sup>1,2</sup> Otherwise, ill-defined structural errors, potentially brought about by kinetic traps, may be unavoidable. However, such a thermodynamic reversibility of the assembly often gives rise to readily deteriorative dynamic nanostructures that are unfavorable for applications. In regard to this contradictory issue, the groups of Raymond<sup>3a</sup> and Fujita<sup>3b,c</sup> reported that, in the formation of large inorganic nanocages, the assembly events at a certain stage change to become hardly dynamic.<sup>3</sup> Compared with such inorganic nanostructures based on metal ion coordination chemistry, nanoscale organic assemblies formed by van der

Waals and  $\pi$ -stacking interactions have been considered more dynamic. Nanotubularly assembled hexabenzocoronene (HBC) derivatives, reported in 2004 by our group,<sup>4–6</sup> provide a typical example of highly elaborate nanostructured organic materials. A prototype of such HBC derivatives carries two triethylene glycol (TEG) chains on one side of the HBC core and two dodecyl side chains on the other (Figure 1).<sup>4</sup> The tubular wall is 3 nm thick

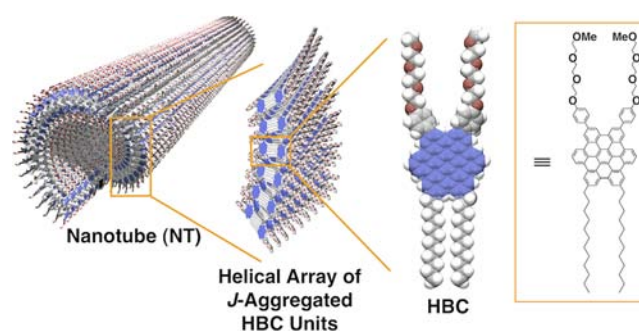


**Figure 1.** Schematic illustration of a nanotubularly assembled hexa-*peri*-hexabenzocoronene (HBC) derivative with a helically rolled-up bilayer wall consisting of *J*-aggregated HBC units.

and consists of a helically rolled-up bilayer assembly of *J*-aggregated HBC units.<sup>5</sup> Consequently, a single nanotube (NT) is chiral with either a left- or right-handed helical geometry.<sup>6</sup> Because of this high level of structural complexity, we have simply thought that the nanotubularly assembled HBC derivatives must be dynamic to a large extent. However, contrary to such a preconceived notion, we report here that the NTs are not dynamic. Instead, the constituent HBC *J*-aggregates carry a high geometrical stability in their helical tubular array.

For the purpose of investigating the dynamic nature of the HBC NTs, we utilized their helical chirality as a probe. In a previous paper,<sup>7</sup> we reported HBC<sup>Py</sup>, an HBC derivative carrying a pyridyl group at the terminus of each TEG chain (Figure 2).

**Received:** December 2, 2012

**Published:** December 19, 2012

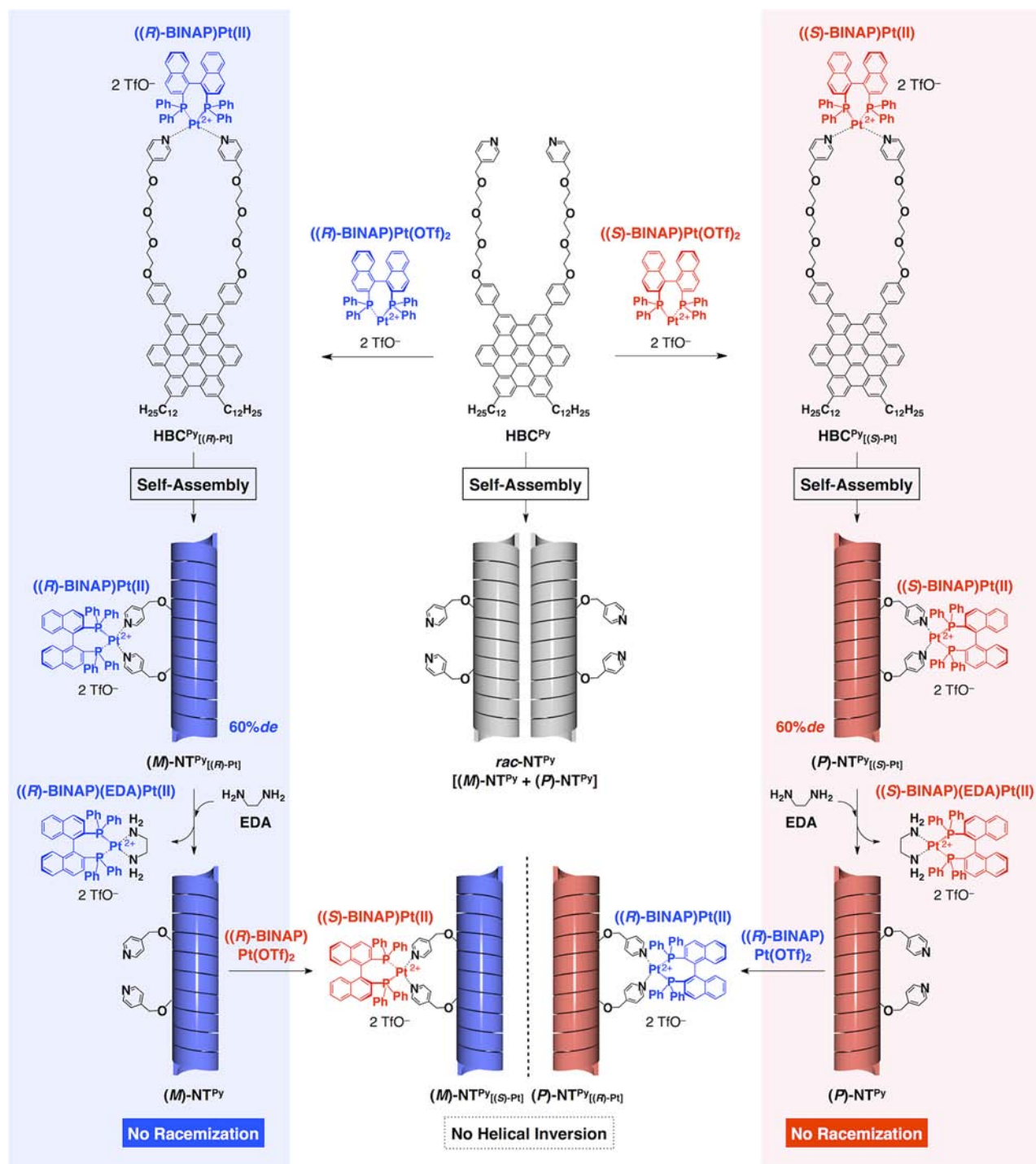


**Figure 2.** Schematic illustration of a series of experiments for investigating the dynamic nature of nanotubularly assembled HBCPy.

Under appropriate conditions, HBCPy can coordinate to a transition-metal ion such as Pt(II) through its pyridyl groups and assemble into NTs.<sup>7</sup> In the present study, HBCPy was allowed to complex with axially chiral (R)- or (S)-BINAPPt(II) with the expectation that the resultant complex HBCPy<sub>[(R)-Pt]</sub> or HBCPy<sub>[(S)-Pt]</sub>, respectively (Figure 2), would self-assemble into one-handed helical NTs, just like the self-assembly of HBC derivatives with chiral oligoether side chains.<sup>6a</sup> In fact, this chiral HBC derivative underwent screw-sense-selective nanotubular self-assembly to form optically active nanotubes NT<sup>Py</sup><sub>[(R)-Pt]</sub> or NT<sup>Py</sup><sub>[(S)-Pt]</sub>. Of particular interest, the nanotubes NT<sup>Py</sup> obtained

by removal of (BINAP)Pt(II) from NT<sup>Py</sup><sub>[(R)-Pt]</sub> or NT<sup>Py</sup><sub>[(S)-Pt]</sub> perfectly maintained their biased helical trajectory even upon heating (Figure 2). The issue of helical memory has been extensively studied by Yashima and co-workers<sup>8</sup> for covalent polymers and by Purrello and co-workers<sup>9a</sup> and Meijer and co-workers<sup>9b-d</sup> for supramolecular polymers composed of  $\pi$ -stacked aromatic motifs.

Chiral HBCPy<sub>[(R)-Pt]</sub> and HBCPy<sub>[(S)-Pt]</sub> (Figure 2) were prepared by the reaction of metal-free HBCPy with Pt(OTf)<sub>2</sub> monohydrate complexes of (R)- and (S)-BINAP, respectively.<sup>10</sup> Next, they were allowed to self-assemble by vapor diffusion.

Typically, a 10 mL vial containing a  $\text{CH}_2\text{Cl}_2$  solution (2 mL) of  $\text{HBC}^{\text{Py}}_{[(R)\text{-Pt}]}$  ( $7.7 \times 10^{-5}$  M) was placed in a 50 mL vial containing ether (8 mL), a poor solvent for  $\text{HBC}^{\text{Py}}_{[(R)\text{-Pt}]}$ . While this setup was kept at 25 °C for 36 h, ether vaporized and diffused into the  $\text{CH}_2\text{Cl}_2$  solution of  $\text{HBC}^{\text{Py}}_{[(R)\text{-Pt}]}$ , whereupon a yellow suspension resulted. Scanning electron microscopy (SEM) of its air-dried sample showed the presence of a large number of bundled nanofibers (Figure S1 in the Supporting Information).<sup>10</sup> We found that this solid substance, which was collected by centrifugation, is well-dispersed in MeOH, affording a clear, yellow-colored dispersion. SEM (Figure 3a) and transmission

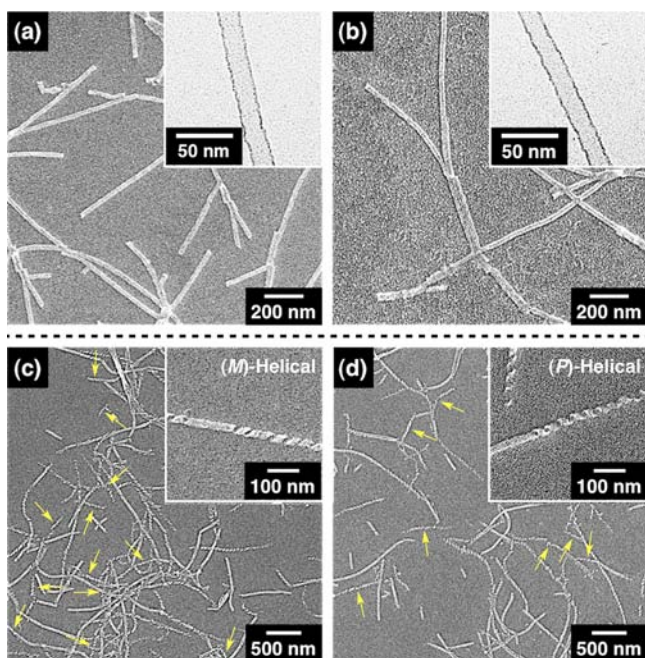


**Figure 3.** (a) SEM and (inset) TEM micrographs of an air-dried dispersion of  $\text{NT}^{\text{Py}}_{[(R)\text{-Pt}]}$  in MeOH. (b) SEM and (inset) TEM micrographs of an air-dried suspension of  $\text{NT}^{\text{Py}}$  in MeOH formed by the removal of the (BINAP)Pt(II) pendants from  $\text{NT}^{\text{Py}}_{[(R)\text{-Pt}]}$ . (c, d) SEM micrographs of mixtures of NCs and NTs formed by self-assembly of (c)  $\text{HBC}^{\text{Py}}_{[(R)\text{-Pt}]}$  and (d)  $\text{HBC}^{\text{Py}}_{[(S)\text{-Pt}]}$  in  $\text{CH}_2\text{Cl}_2$  upon diffusion of MeOH vapor. The insets in (c) and (d) highlight NTs partially exfoliated into NC strands. The yellow arrows point out NCs with a minor helical sense.  $[M]:[P] = 48:12$  and  $7:26$  in (c) and (d), respectively.

electron microscopy (TEM) (Figure S2a and Figure 3a inset)<sup>10</sup> of its air-dried sample visualized the presence of  $\text{NT}^{\text{Py}}_{[(R)\text{-Pt}]}$  with a uniform diameter of 18 nm and a wall thickness of 3 nm (for  $\text{NT}^{\text{Py}}_{[(S)\text{-Pt}]}$ , see Figure S3a,b).<sup>10</sup> Because  $\text{HBC}^{\text{Py}}_{[(R)\text{-Pt}]}$  itself, unless tubularly assembled, is insoluble in MeOH, the enhanced dispersibility of  $\text{NT}^{\text{Py}}_{[(R)\text{-Pt}]}$  can be attributed to its cationic metal ion pendants that fully cover the NT surface.<sup>4c,11</sup>

As commonly observed for tubularly assembled HBC derivatives, the MeOH dispersion of  $\text{NT}^{\text{Py}}_{[(R)\text{-Pt}]}$  at 25 °C displayed an electronic absorption spectrum with two red-shifted absorption bands at 430 and 459 nm (Figure S4, blue curve),<sup>10</sup> characteristic of J-aggregated HBC units.<sup>4,5</sup> In this visible absorption region,  $\text{NT}^{\text{Py}}_{[(R)\text{-Pt}]}$  in MeOH showed two distinct circular dichroism (CD) bands at 430 and 459 nm (Figure 4b, blue curve). The CD spectrum thus observed was a perfect mirror image of that of  $\text{NT}^{\text{Py}}_{[(S)\text{-Pt}]}$  obtained by the assembly of  $\text{HBC}^{\text{Py}}_{[(S)\text{-Pt}]}$  (Figure 4b; red curve). It should be noted that nonassembled  $\text{HBC}^{\text{Py}}_{[(R)\text{-Pt}]}$  in  $\text{CH}_2\text{Cl}_2$  displayed CD bands only

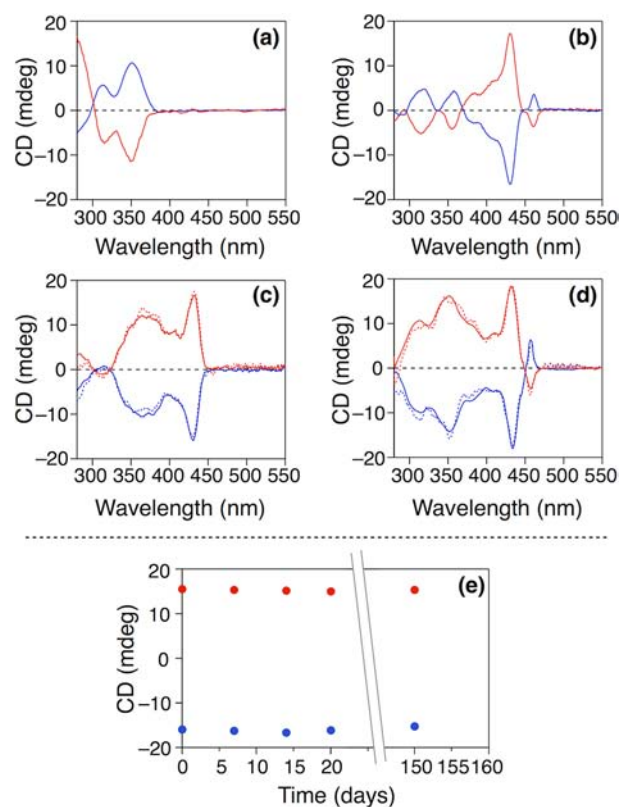


**Figure 4.** (a) CD spectra of  $\text{HBC}^{\text{Py}}_{[(R)\text{-Pt}]}$  (blue curve) and  $\text{HBC}^{\text{Py}}_{[(S)\text{-Pt}]}$  (red curve) in  $\text{CH}_2\text{Cl}_2$  at 25 °C. (b) CD spectra of  $\text{NT}^{\text{Py}}_{[(R)\text{-Pt}]}$  (blue curve) and  $\text{NT}^{\text{Py}}_{[(S)\text{-Pt}]}$  (red curve) in MeOH at 25 °C. (c) CD spectra (MeOH, 25 °C) of  $\text{NT}^{\text{Py}}$  derived from  $\text{NT}^{\text{Py}}_{[(R)\text{-Pt}]}$  (blue solid curve) or  $\text{NT}^{\text{Py}}_{[(S)\text{-Pt}]}$  (red solid curve) upon removal of the (BINAP)Pt(II) pendants using EDA ( $[\text{EDA}]:[\text{HBC}^{\text{Py}}] = 600:1$ , 2 h). Dotted curves represent the CD spectra after heating at 50 °C for 12 h. (d) CD spectra (MeOH, 25 °C) after mixing  $\text{NT}^{\text{Py}}$  derived from  $\text{NT}^{\text{Py}}_{[(R)\text{-Pt}]}$  with (S)- (BINAP)Pt(II)(OTf)<sub>2</sub> (blue solid curve) or  $\text{NT}^{\text{Py}}$  derived from  $\text{NT}^{\text{Py}}_{[(S)\text{-Pt}]}$  with (R)- (BINAP)Pt(II)(OTf)<sub>2</sub> (red solid curve) at a  $[(\text{BINAP})\text{Pt}(\text{II})]:[\text{HBC}^{\text{Py}}]$  ratio of 1:1. The dotted curves show CD spectra recorded 5 months after mixing at 25 °C. (e) CD intensity changes at 430 nm from (d) with time. All of the CD spectra were recorded at  $[\text{HBC}^{\text{Py}}] = 7.7 \times 10^{-5}$  M.

at 315 and 352 nm (Figure 4a, blue curve) due to the axially chiral (BINAP)Pt(II) pendants bound to the pyridyl groups (Figure S5b, blue curve).<sup>10</sup> Therefore, the chiroptical activity of  $\text{NT}^{\text{Py}}_{[(R)\text{-Pt}]}$  in its visible absorption region indicates that the nanotubular helical assembly of  $\text{HBC}^{\text{Py}}_{[(R)\text{-Pt}]}$  is either left-handed-enriched, (M)- $\text{NT}^{\text{Py}}_{[(R)\text{-Pt}]}$ , or right-handed-enriched, (P)- $\text{NT}^{\text{Py}}_{[(R)\text{-Pt}]}$  (Figure 2). It is noteworthy that when MeOH was used instead of ether for the self-assembly of  $\text{HBC}^{\text{Py}}_{[(R)\text{-Pt}]}$  under vapor-diffusion conditions, helical nanocoils (NCs) were formed along with the NTs (Figure 3c). The NCs (Figure 3c inset) can be regarded as a structurally relaxed form of  $\text{NT}^{\text{Py}}_{[(R)\text{-Pt}]}$ .<sup>6b</sup> From arbitrarily selected SEM micrographs, we confirmed that roughly 80% of the observed NCs adopted an (M)-helical sense [60% diastereomeric excess (de)]. As expected,  $\text{HBC}^{\text{Py}}_{[(S)\text{-Pt}]}$  with the opposite configuration of the BINAP pendant predominantly gave rise to (P)-helical NCs (Figure 3d and its inset), again with 60% de. The observed selectivity is remarkable considering that the chiral pendant is attached to the assembling aromatic core by the rather long (>1 nm) and flexible spacer.

The (BINAP)Pt(II) pendants could be detached from the NT surface by treatment with an excess amount of ethylenediamine (EDA) (Figure 2). Typically, EDA was added to a MeOH dispersion of NT<sup>Py</sup><sub>[(R)-Pt]</sub> ([HBC<sup>Py</sup><sub>[(R)-Pt]</sub>] = 5.1 × 10<sup>-5</sup> M; [EDA] = 0.03 M), and the mixture was gently stirred at 25 °C for 2 h in the dark. The resulting yellow suspension was subjected to centrifugation, and the resultant precipitate was collected and washed three times with a MeOH solution (2 mL) of EDA (0.1 M). By means of SEM (Figure 3b) and TEM (Figure S2b and Figure 3b inset),<sup>10</sup> we confirmed that the solid substance thus isolated was composed exclusively of NTs with diameter (18 nm) and wall thickness (3 nm) nearly identical to those of the NT<sup>Py</sup><sub>[(R)-Pt]</sub> precursor (Figure 3a). No residual (BINAP)Pt(II) was detected by <sup>1</sup>H NMR spectroscopy and elemental analysis, indicating that the chiral pendants were completely removed from the inner and outer surfaces of NT<sup>Py</sup><sub>[(R)-Pt]</sub> (Figure 2). Accordingly, this transformation was accompanied by a slight decrease in intensity of the broad absorption band centered at 365 nm. However, the absorption intensities of the resultant NT<sup>Py</sup> at 430 and 459 nm due to the *J*-aggregated HBC units remained unchanged (Figure S6).<sup>10</sup>

Because of the presence of chiral elements in the helical HBC array and its surface pendants, (*M*)-NT<sup>Py</sup><sub>[(R)-Pt]</sub> and (*P*)-NT<sup>Py</sup><sub>[(R)-Pt]</sub> are diastereoisomers of one another (Figure 2). However, (*M*)-NT<sup>Py</sup> and (*P*)-NT<sup>Py</sup> derived from them by removal of the (BINAP)Pt(II) pendants are enantiomers.<sup>8,9</sup> Hence, if the helical HBC array in NT<sup>Py</sup> were highly dynamic, (*M*)-NT<sup>Py</sup>, for example, could eventually be racemized to give an optically inactive 1:1 mixture of (*M*)-NT<sup>Py</sup> and (*P*)-NT<sup>Py</sup>. However, NT<sup>Py</sup> obtained from NT<sup>Py</sup><sub>[(R)-Pt]</sub> remained optically active (Figure 2). As shown by the blue solid curve in Figure 4c, the CD intensity at 430 nm in MeOH was essentially identical to that observed for its precursor NT<sup>Py</sup><sub>[(R)-Pt]</sub> (Figure 4b, blue curve). Although a significant CD spectral change took place at 300–400 nm, this change is reasonable when the CD spectral profile of pyridine-coordinated (*R*)-(BINAP)(Py)<sub>2</sub>Pt(II) (Figure S5b, blue curve) is taken into account. An analogous CD spectral change was observed for the transformation of NT<sup>Py</sup><sub>[(S)-Pt]</sub> (Figure 4b, red curve) into NT<sup>Py</sup> (Figure 4c, red solid curve). Interestingly, even upon heating for 12 h at 50 °C, the chiroptical activity thus observed for NT<sup>Py</sup> was maintained without any decrease in CD intensity (Figure 4c, dotted curves). These observations demonstrate a high thermal stability of the helical HBC array in NT<sup>Py</sup>. Just in case, we added (*S*)-(BINAP)Pt(II)(OTf)<sub>2</sub> to NT<sup>Py</sup> derived from NT<sup>Py</sup><sub>[(R)-Pt]</sub> at a [(BINAP)Pt(II)]:[HBC<sup>Py</sup>] ratio of 1:1 in MeOH (Figure 2). The mixture immediately showed the expected CD spectral change at 300–400 nm (Figure 4d, blue solid curve) for the complexation of NT<sup>Py</sup> with (*S*)-(BINAP)Pt(II), matching the CD spectral profile of its pyridyl complex (Figure S5b, red curve). However, even over a period of 5 months, the CD band at 430 nm did not show any appreciable change associated with helical inversion of the HBC array (Figure 4d,e).<sup>12</sup>

In conclusion, by using (BINAP)Pt(II) as a detachable chiral auxiliary for the non-covalent assembly of a hexabenzocoronene derivative, HBC<sup>Py</sup>, we succeeded in the first asymmetric synthesis of a highly elaborate “nanotubular” helical architecture (Figure 1) with 60% de (80:20 diastereomeric ratio). In view of the rather long (>1 nm) and flexible spacer between the chiral auxiliary and the HBC core, the assembly event is highly sensitive stereochemically. The optically active NTs obtained after the removal of the detachable chiral auxiliary (Figure 2) did not racemize over a period of >5 months, demonstrating a large geometrical

stability of the *J*-aggregated HBC units in the NT. Why then can this poorly dynamic molecular assembly fulfill the large stereochemical requisite for the formation of such an elaborate nanotubular architecture? We suppose that the assembly event is analogous to that of crystallization, where only the growing termini of the NT are dynamic, allowing the correction of any kinetically driven geometrical errors that may be generated.

## ■ ASSOCIATED CONTENT

### ● Supporting Information

Synthesis details; NMR, electronic absorption, and CD spectra; and SEM and TEM images. This material is available free of charge via the Internet at <http://pubs.acs.org>.

## ■ AUTHOR INFORMATION

### Corresponding Author

fukushima@res.titech.ac.jp; aida@macro.t.u-tokyo.ac.jp

### Notes

The authors declare no competing financial interest.

## ■ ACKNOWLEDGMENTS

W.Z. thanks the Japan Society for the Promotion of Science for a Young Scientists Fellowship (21-9925).

## ■ REFERENCES

- (1) Aida, T.; Meijer, E. W.; Stupp, S. I. *Science* **2012**, *335*, 813.
- (2) (a) Brunsveld, L.; Folmer, B. J. B.; Meijer, E. W.; Sijbesma, R. P. *Chem. Rev.* **2001**, *101*, 4071. (b) Purrello, R. *Nat. Mater.* **2003**, *2*, 216. (c) Hoeven, F. J. M.; Jonkheijm, P.; Meijer, E. W.; Schenning, A. P. H. J. *Chem. Rev.* **2005**, *105*, 1491. (d) De Greef, T. F. A.; Smulders, M. M. J.; Wolfs, M.; Schenning, A. P. H. J.; Sijbesma, R. P.; Meijer, E. W. *Chem. Rev.* **2009**, *109*, 5687.
- (3) (a) Davis, A. V.; Fiedler, D.; Ziegler, M.; Terpin, A.; Raymond, K. N. *J. Am. Chem. Soc.* **2007**, *129*, 15354. (b) Sato, S.; Ishido, Y.; Fujita, M. *J. Am. Chem. Soc.* **2009**, *131*, 6064. (c) Fujita, D.; Takahashi, A.; Sato, S.; Fujita, M. *J. Am. Chem. Soc.* **2011**, *133*, 13317.
- (4) (a) Hill, J. P.; Jin, W.; Kosaka, A.; Fukushima, T.; Ichihara, H.; Shimomura, T.; Ito, K.; Hashizume, T.; Ishii, N.; Aida, T. *Science* **2004**, *304*, 1481. (b) Yamamoto, Y.; Fukushima, T.; Suna, Y.; Ishii, N.; Saeki, A.; Seki, S.; Tagawa, S.; Taniguchi, M.; Kawai, T.; Aida, T. *Science* **2006**, *314*, 1761. (c) Zhang, W.; Jin, W.; Fukushima, T.; Saeki, A.; Seki, S.; Aida, T. *Science* **2011**, *334*, 340.
- (5) Jin, W.; Yamamoto, Y.; Fukushima, T.; Ishii, N.; Kim, J.; Kato, K.; Takata, M.; Aida, T. *J. Am. Chem. Soc.* **2008**, *130*, 9434.
- (6) (a) Jin, W.; Fukushima, T.; Niki, M.; Kosaka, A.; Ishii, N.; Aida, T. *Proc. Natl. Acad. Sci. U.S.A.* **2005**, *102*, 10801. (b) Yamamoto, T.; Fukushima, T.; Yamamoto, Y.; Kosaka, A.; Jin, W.; Ishii, N.; Aida, T. *J. Am. Chem. Soc.* **2006**, *128*, 14337.
- (7) Zhang, W.; Jin, W.; Fukushima, T.; Ishii, N.; Aida, T. *Angew. Chem., Int. Ed.* **2009**, *48*, 4747.
- (8) Yashima, E.; Maeda, K.; Iida, H.; Furusho, Y.; Nagai, K. *Chem. Rev.* **2009**, *109*, 6102.
- (9) (a) Bellacchio, E.; Lauceri, R.; Gurrieri, S.; Scolaro, L. M.; Romeo, A.; Purrello, R. *J. Am. Chem. Soc.* **1998**, *120*, 12353. (b) Helmich, F.; Lee, C. C.; Schenning, A. P. H. J.; Meijer, E. W. *J. Am. Chem. Soc.* **2010**, *132*, 16753. (c) Helmich, F.; Smulders, M. M. J.; Lee, C. C.; Schenning, A. P. H. J.; Meijer, E. W. *J. Am. Chem. Soc.* **2011**, *133*, 12238. (d) George, S. J.; Bruijn, R.; Tomović, Z.; Averbeke, B. V.; Beljonne, D.; Lazzaroni, R.; Schenning, A. P. H. J.; Meijer, E. W. *J. Am. Chem. Soc.* **2012**, *134*, 17789.
- (10) See the Supporting Information.
- (11) Zhang, G.; Jin, W.; Fukushima, T.; Kosaka, A.; Ishii, N.; Aida, T. *J. Am. Chem. Soc.* **2007**, *129*, 719.
- (12) No enantioselective complexation took place between helically enriched NT<sup>Py</sup> derived from NT<sup>Py</sup><sub>[(R)-Pt]</sub> and *rac*-(BINAP)Pt(II)(OTf)<sub>2</sub> in MeOH at 25 °C.